

Static frequency tuning accounts for changes in neural synchrony evoked by transient communication signals

Henriette Walz,¹ Jan Grewe,^{1,2} and Jan Benda²

¹Bernstein Center for Computational Neuroscience Munich, Planegg-Martinsried, Germany; and ²Neuroethology, Institute for Neurobiology, University of Tübingen, Tübingen, Germany

Submitted 13 August 2013; accepted in final form 20 May 2014

Walz H, Grewe J, Benda J. Static frequency tuning accounts for changes in neural synchrony evoked by transient communication signals. *J Neurophysiol* 112: 752–765, 2014. First published May 21, 2014; doi:10.1152/jn.00576.2013.—Although communication signals often vary continuously on the underlying signal parameter, they are perceived as distinct categories. We here report the opposite case where an electrocommunication signal is encoded in four distinct regimes, although the behavior described to date does not show distinct categories. In particular, we studied the encoding of chirps by P-unit afferents in the weakly electric fish *Apteronotus leptorhynchus*. These fish generate an electric organ discharge that oscillates at a certain individual-specific frequency. The interaction of two fish in communication contexts leads to the emergence of a beating amplitude modulation (AM) at the frequency difference between the two individual signals. This frequency difference represents the social context of the encounter. Chirps are transient increases of the fish's frequency leading to transient changes in the frequency of the AM. We stimulated the cells with the same chirp on different, naturally occurring background beats. The P-units responded either by synchronization or desynchronization depending on the background. Although the duration of a chirp is often shorter than a full cycle of the AM it elicits, the distinct responses of the P-units to the chirp can be predicted solely from the frequency of the AM based on the static frequency tuning of the cells.

communication signals; sensory coding; spike synchrony; weakly electric fish

THE CORRECT DECODING OF COMMUNICATION signals in aggressive and mating contexts is crucial to an animal's survival and reproductive success. Not surprisingly, the perception of communication signals happens robustly, even though their characteristic features often only last milliseconds (e.g., Vernaleo and Dooling 2011; Salgado and Zupanc 2011). Many acoustic as well as electric signals include frequency sweeps and modulations in a variety of vertebrate species ranging from fish (Zakon et al. 2002) over bats (Siemers and Schnitzler 2004) to primates (Wang et al. 1995) and humans (Liberman and Mattingly 1989). They often occur in social situations in which interfering signals from different individuals (Cherry 1953; Zupanc and Maler 1993; McKibben and Bass 1998) make decoding particularly hard.

Albeit often consisting of continuously variable acoustic signals, communication signals are perceived as distinct categories (e.g., in humans, Holt and Lotto 2010; monkeys, May et al. 1989; or birds, Nelson and Marler 1989). Recent studies have revealed neural correlates of this mapping from variable

sensory stimuli to perceptual categories (Prather et al. 2009; Gifford et al. 2005). Here we find that, on the level of electroreceptor units, the same electrocommunication signal is encoded in four different regimes of beat frequencies. This distinction is not reflected by corresponding behavioral categories. A socially relevant background signal that interacts with the electrocommunication signal has previously been found to continuously influence communication behavior (Bastian et al. 2001; Hupé et al. 2008; Walz et al. 2013).

Weakly electric fish emit an electric organ discharge (EOD) that they use for navigation and communication purposes. Their EOD oscillates at an individual-specific frequency that is stable under baseline conditions but modulated in the context of communication (Moortgat et al. 1998; Zakon et al. 2002). The electrocommunication signal we focus on is the so-called small (type-2) chirp (Hagedorn and Heiligenberg 1985; Dye 1987). During such a chirp, the emitting fish transiently increases the EOD frequency (EODf) by ~100 Hz for a few tens of milliseconds. As a result the EOD amplitude of the emitting and perceiving fish is modulated depending on the background beat frequency that equals the frequency difference between the two EODf (Zupanc and Maler 1993; Benda et al. 2005; Walz et al. 2013). Different beat signals resemble different social encounters, because the EODf depends on gender (Meyer et al. 1987; Zakon and Dunlap 1999) and size (Triefenbach and Zakon 2008; Fugère et al. 2011) of the fish. The beat frequency therefore potentially reflects how different the fish are in these aspects. The beat also influences chirp production with more chirps being produced at lower beat frequencies (Engler and Zupanc 2001; Bastian et al. 2001; Hupé et al. 2008).

Amplitude modulations (AMs) such as beats and chirps are primarily encoded by P-type electroreceptor afferents. These neurons fire phase-locked action potentials to each EOD cycle with a probability that depends both on the amplitude and the frequency of AMs. P units show strong spike-frequency adaptation and thus reduced responses to slow AM frequencies. Chirps transiently increase the AM frequency, release the P-units from adaptation, and increase their response when emitted on low beat frequencies (Benda et al. 2005). However, as we show, the P-unit response differs when chirps occur on other beat frequencies.

We start out with describing the signals chirps elicit at different background beats. Our single unit as well as whole nerve recordings demonstrate that the chirp either synchronizes or desynchronizes the population of P-unit receptor afferents depending on the beat frequency. This results in a division of the representation of the chirp on the receptor level into four

Address for reprint requests and other correspondence: J. Benda, Institute for Neurobiology, Univ. of Tübingen, 72076 Tübingen, Germany (e-mail: jan.benda@uni-tuebingen.de).

coding regimes. We finally demonstrate that the rapid responses of the cells to chirps can be well predicted based on their frequency tuning curves and that the position of the chirps within the beat only plays a role at low beat frequencies.

MATERIALS AND METHODS

In vivo electrophysiology. Intracellular as well as whole nerve recordings were made from the anterior part of the lateral line nerve of 52 brown ghost knifefish (*Apteronotus leptorhynchus*, *Gymnotiformes*) of either sex (46 for intracellular and 6 for whole nerve recordings, 12- to 16-cm body length, EOD frequency between 602 and $948,767 \pm 97$ Hz).

First, fish were anesthetized with MS-222 (120 mg/l; PharmaQ, Fordingbridge, UK) and a small part of the skin was removed atop of the lateral line just behind the skull. Right after surgery and throughout the entire electrophysiological experiment the margin of the wound was regularly treated by local anesthetics Lidocaine (2%; bela-pharm, Vechta, Germany). The nerve was not affected by this treatment since we found no difference between recordings from the nerve and recordings from the deep fiber layer in the electrosensory lateral line lobe (ELL; Benda et al. 2005, 2006). For the recordings fish were immobilized (Tubocurarine; Sigma-Aldrich, Steinheim, Germany; 25–50 μ l of 5 mg/ml solution), placed in a tank, and respired by a constant flow of water through their mouth. The water in the experimental tank ($47 \times 42 \times 12$ cm) was from the fish's home tank with a conductivity of ~ 300 μ S/cm and kept at 28°C. All experimental protocols were approved and complied with national and regional laws (file no. 55.2-1-54-2531-135-09).

For intracellular recordings of P-unit afferents, we used standard glass microelectrodes (borosilicate; 1.5-mm outer diameter; GB150F-8P; Science Products, Hofheim, Germany) pulled to a resistance of 50–100 M Ω (model P-97; Sutter Instrument, Novato, CA) and filled with a 1-M KCl solution. Electrodes were advanced into the nerve using microdrives (Luigs-Neumann, Ratingen, Germany). Potentials were recorded using the bridge mode of the SEC-05 amplifier (npi electronics, Tamm, Germany) and low-pass filtered at 10 kHz.

Spikes were detected online as peaks that exceeded a dynamically adjusted threshold value above the previous detected trough (Todd and Andrews 1999). To track changes in amplitude of the recorded spikes, the threshold was set to 50% of the amplitude of a detected spike but not below a minimum threshold that was set above the noise in the recording based on a histogram of all peak amplitudes. Trials with bad spike detection were discarded from further offline analysis.

Population activity in whole nerve recordings was measured using a pair of hook electrodes of chlorided silver wire. Recorded signals were differentially amplified (gain between 200 and 2,000) and band-pass filtered (2- to 5,000-Hz passband, DPA2-FX; npi electronics). The strong EOD artifact in this kind of recording was eliminated before further analysis by applying a running average of the size of one EOD period (Benda et al. 2006).

The EOD of the fish was recorded between its head and tail using a pair of vertical carbon rods (11-cm long, 8-mm diameter), amplified 200–500 times and band-pass filtered (3- to 1,500-Hz passband, DPA2-FX; npi electronics). These electrodes were placed isopotential to the stimulus field (see below) to eliminate contamination with the stimulus. During electrophysiological experiments, the actual stimulus driving the receptor cells was estimated by recording the voltage between a pair of silver wires (1 cm apart) placed perpendicular to the trunk of the fish, thus approximating the transdermal voltage (amplification 200–500 times, band-pass filtered with 3- to 1,500-Hz passband, DPA2-FX; npi electronics).

For online spike and EOD detection, stimulus generation and calibration, as well as preanalysis and visualization of the data, we used the ephys, efield, and efish plugin sets of the software RELACS (www.relacs.net) running on a Debian Linux computer. All recorded

data were digitized using a data acquisition board (PCI-6229; National Instruments, Austin, TX) at a sampling rate of 20 kHz.

Electrosensory stimulation. During experiments, the electrosensory scene representing different encounters with other fish was created by electrical stimulation. The stimuli were applied using a pair of stimulation electrodes (carbon rods, 30-cm long, 8-mm diameter) placed on either side of the fish parallel to its longitudinal axis. Stimuli were computer-generated and passed to the stimulation electrodes after being attenuated to the right amplitude and isolated from ground (Attenuator: ATN-01M; Isolator: ISO-02V; npi electronics).

The EOD of a second fish can be mimicked by stimulating directly with a sine wave of an appropriate amplitude and frequency. The superposition of this stimulus with the EOD of the fish from which we recorded results in a beat, a periodic AM with a frequency given by the difference between the frequencies of the stimulus and the EOD of the fish, the “difference frequency” Δf_{Beat} , and an amplitude A that we set to 10 or 20% of the amplitude of the fish's EOD. In addition, chirps can be mimicked by Gaussian frequency and AM of the stimulating sine wave. The time-dependent frequency difference $\Delta f(t)$ between stimulus and EODf then follows

$$\Delta f(t) = \Delta f_{\text{Beat}} + s \cdot \exp\left(-\frac{t^2}{2\sigma^2}\right), \quad (1)$$

where Δf_{Beat} is the difference frequency of the underlying beat, s is the maximal frequency excursion during the chirp (its size), and $\sigma = \Delta t / \sqrt{2 \ln 10}$ sets the width of the chirp, Δt , at 10% height of the Gaussian modulation. We used chirps of $s = 60$ or 100 Hz and $\Delta t = 14$ ms. The amplitude of the EOD of the emitting fish was decreased by a Gaussian of the same width by maximally 2% of the baseline amplitude (see Fig. 1 for a schema of a small chirp). The sine wave stimulus including the chirp leads to a specific AM of the EOD with a frequency following Eq. 1 that is encoded by the P units.

Alternatively to stimulation with an EOD mimic, any AM can be obtained by multiplying the intended AM with the fish's own EOD (multiplier: MXS-01M; npi electronics) and playing the multiplied signal back via the stimulation electrodes.

To generate the AM resulting from the superposition of the EOD of a fish emitting a chirp at time $t = 0$ and a receiving fish, we computed the AM according to

$$\text{AM}(t) = A(t) \cos[\Delta\phi(t)], \quad (2)$$

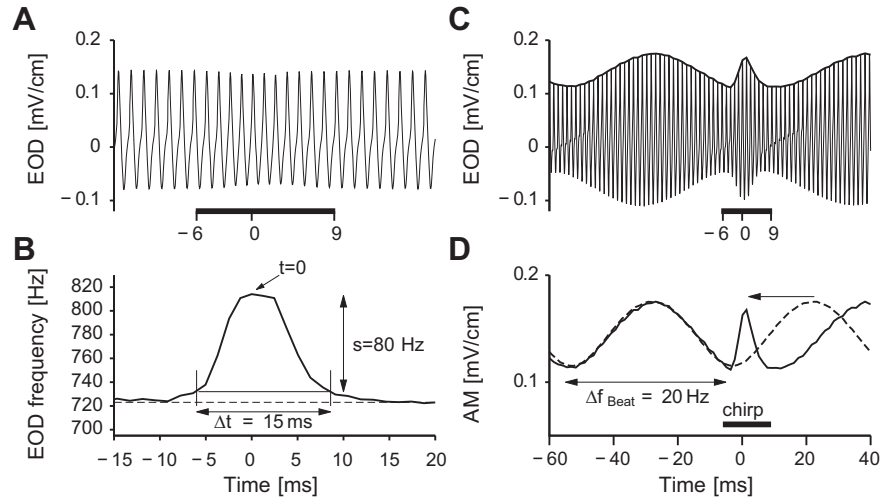
where

$$\Delta\phi(t) = 2\pi \int_{-\infty}^t \Delta f(t') dt' = 2\pi \Delta f_{\text{Beat}} t + 2\pi s \sigma \int_{-\infty}^{t/\sigma} \exp(-z^2) dz + \Delta\phi_0, \quad (3)$$

is the phase of the beat as the time integral over the frequency difference of the two EODs. The first term models the beat resulting from the superposition of the two EODs with the difference frequency Δf_{Beat} . The second term accounts for the Gaussian increase of the frequency difference during the chirp. $\Delta\phi_0$ determines the phase of the beat cycle at which the chirp occurs; it is zero at the peak of a beat cycle. In addition, the EOD amplitude $A(t)$ was decreased by multiplying it with a Gaussian kernel of the same width and centered at time $t = 0$ by 2%.

A single stimulus of a given difference frequency was composed of chirps at 10 different phases of the beat (every 36°). At least 200 ms or one beat period, whichever was larger, separated the chirps. Each such stimulus of 10 chirps was repeated 16 times. Then, the next stimulus with a different difference frequency, contrast, or chirp size was played. After being recorded, chirps evoked by the same stimulus were grouped according to the measured phase of the beat at which they occurred. Because of slight changes in EODf of the fish, the phase of a chirp within a beat cycle can vary when using direct stimulation, so that instead of exactly 16 we got between 10 and 20 responses to each chirp of a given phase.

Fig. 1. A small chirp and its effect on the amplitude modulation sensed by a receiving fish. *A*: electric organ discharge (EOD) waveform of a single fish during a small chirp. The largest frequency excursion of the chirp is at *time 0* (arrow in *B*). Chirp beginning and end are defined as the times the EOD frequency (EODf) excursion exceeds 10% of the chirp size *s* and are indicated by tick marks and black bar. *B*: EOD frequency during the chirp; *s* is the maximum deviation from baseline EODf (vertical arrow). The horizontal arrow shows the chirp width. *C*: resulting EOD waveform close to a receiving fish that has an EODf of 20 Hz below the chirping fish (thin line) and its amplitude modulation (AM; thick line). The chirp alters the AM form (black bar). *D*: without the chirp the AM would be an ongoing beat (dashed line) with frequency given by the difference, Δf_{beat} , of the 2 EODfs. The chirp (black bar) transiently increases $\Delta f(t)$ for less than a full period of the beat (solid line).



Both the direct and the AM stimuli primarily elicit responses in P-unit electroreceptors. Since we found no differences in the evoked effects on the cells, data from both stimulation paradigms were pooled (Benda et al. 2005). We also pooled data over both contrasts used (10 and 20%), since we did not obtain different results when analyzed separately.

Chirp encoding analysis. The time course of the firing rate (the peristimulus time histograms) was computed by convolving each spike train with a Gaussian kernel with a standard deviation of 1 ms and averaging over trials. We chose 1 ms as our default kernel since it corresponds to the fast excitatory component of postsynaptic potentials evoked by P-units in their target cells, the pyramidal cells in the ELL (Berman and Maler 1998). We also tested different kernel widths and found small quantitative but no qualitative differences (not shown).

We calculated the response during beat and chirp by averaging within two time windows, one located during the beat before the presentation of a chirp and the other one centered around the chirp. For the size of the analysis window for responses to the beat, we took the largest integer multiple of the beat period smaller than 60 ms but at least one full beat period for beat cycles longer than 60 ms. The window for chirp response analysis spanned the width of the chirp stimulus (14 ms) stretched by a factor of 1.2 and was shifted by 5 ms with respect to the time of stimulus application to account for neuronal delays. The firing rate response in each time window was assessed as the modulation depth of the firing rate, i.e., the standard deviation of the peristimulus time histograms. The population activity recorded from the lateral line nerve was similarly assessed by calculating the standard deviation of the recorded voltage.

The average correlation between pairs (*i*, *j*) of spike trains, as a measure of synchrony, was quantified by means of the correlation coefficient

$$r_{ij} = \frac{\langle (s_i - \langle s_i \rangle_t) (s_j - \langle s_j \rangle_t) \rangle_t}{\sqrt{\langle (s_i - \langle s_i \rangle_t)^2 \rangle_t} \sqrt{\langle (s_j - \langle s_j \rangle_t)^2 \rangle_t}} \quad (4)$$

where s_i and s_j are two spike trains convolved with a Gaussian kernel with a standard deviation of 1 ms (see above) and $\langle \dots \rangle_t$ denotes averaging over time. The r_{ij} are then averaged over all possible pairs of spike trains recorded in one cell in response to a specific stimulus.

To assess the effect of chirps at different beats, we calculated the chirp selectivity index (CSI; see Vonderschen and Chacron 2011) as

$$\text{CSI} = \frac{r_{\text{chirp}} - r_{\text{beat}}}{r_{\text{chirp}} + r_{\text{beat}}} \quad (5)$$

where r_{chirp} is the response (standard deviation of the firing rate or of the population activity, or spike-train correlation) during the chirp and

r_{beat} is the response during the beat. The CSI is greater than zero when chirps increase the response of a cell and less than zero if they decrease the response relative to the response evoked by the beat. Note that the CSI yields qualitatively similar results to that of the chirp gain ($r_{\text{chirp}}/r_{\text{beat}}$) used in previous studies (Benda et al. 2005, 2006).

We also predicted the CSI solely from the responses of P-units to beats, i.e., their AM frequency tuning. This analysis is based on the simplifying assumption that P-units only respond to the frequency change of the AM caused by the chirp. For the predictions we first calculated the mean frequency excursion of the chirp, which is 60 Hz in the case of a chirp of $s = 100$ Hz. We then predicted the response to the chirp to be similar to the response to a beat that is 60 Hz higher than the underlying background beat. The predicted CSI was subsequently calculated between the response to the beat of the frequency elicited by the chirp (60 Hz above underlying beat frequency) and the response to the underlying beat. The predictions were calculated from the tuning curves of single nerves, which were averaged over different trials.

Chirp discrimination analysis. The distance between two spike trains was quantified using a spike train metric according to

$$d^2(s_i, s_j)_{\tau_c} = \frac{1}{\tau_c} \int_{t_1}^{t_2} [s_i - s_j]^2 dt \quad (6)$$

where s_i and s_j are two spike trains convolved with an alpha-function of width τ_c that we varied from 1 to 100 ms (van Rossum 2001). We examined P-unit responses on two different integration intervals: one ranging from $t_1 = -10$ ms to $t_2 = 25$ ms that contained the chirp response only (as in Marsat and Maler 2010), while the other ranging from $t_1 = -10$ ms to $t_2 = 100$ ms in addition contained the beat context (as in Vonderschen and Chacron 2011).

We then asked whether the spike trains evoked by chirps occurring on different phases in the beat are distinguishable. For this we grouped all spike trains evoked by a chirp of a specific size according to the phase $\Delta\phi_0$ in the beat where the chirp occurred into $n = 10$ phase bins indexed by *a*, each bin covering 36° . We then took each spike train, computed its average distance (Eq. 6) to all the spike trains of each of the bins and incremented the number of assigned spike trains in that bin *b* with the minimal average distance to the spike train by one. Chirps occurring in different phases of the beat would be optimally distinguishable if each spike train was assigned to the same phase bin it originated from. From this procedure we constructed confusion matrices $p(a, b)$ by counting the number of spike trains originating from phase bin *a* and assigned to phase bin *b* for all n^2 combinations of phase bins *a* and *b* and normalizing by the total number of spike trains. The confusion matrices were averaged over all cells. In case of optimal distinction, this matrix only had values different from zero on

the diagonal where $a = b$. The less well different phases could be distinguished the more off-diagonal elements would carry significant entries.

The discriminability can be quantified by the mutual information I contained in this confusion matrix, which is calculated according to

$$I = \sum_{a=1}^n \sum_{b=1}^n p(a, b) \log_2 \frac{p(a, b)}{p(a) \cdot p(b)} \quad (7)$$

where $p(a)$ is the fraction of trials in which the chirp was delivered at a beat phase falling into phase bin a and $p(b)$ is the fraction of spike trains that was assigned as having been evoked by beat phase in bin b . $p(a, b)$ is the fraction of responses that were assigned to beat phase b , although having been elicited by a . We normalized the mutual information by its maximum possible value $I_{\max} = -\sum_{a=1}^n p(a) \log_2 p(a)$, the entropy of the stimulus, such that the relative mutual information

$$I_{\text{rel}} = \frac{I}{I_{\max}} \quad (8)$$

ranges from zero to one, with higher values indicating better discriminability.

RESULTS

EOD AMs caused by small chirps. Small chirps (Engler et al. 2000) are short EOD modulations of a small Gaussian-shaped frequency excursion ranging from a few tens up to ~ 150 Hz (the size of a chirp s) and lasting for around 10–20 ms (its width Δt ; Engler et al. 2000; Engler and Zupanc 2001; Bastian et al. 2001; Kolodziejski et al. 2007; see Fig. 1, *A* and *B*). The superposition of two EODs leads to a regular AM, i.e., the beat. At a receiving fish, a chirp causes a characteristic disruption of the regular beat pattern (Fig. 1*C*), for example, a brief acceleration (Fig. 1*D*).

However, the AM caused by a chirp strongly depends on the difference frequency of the underlying beat, Δf_{Beat} , indicating the social context, as well as on the phase, $\Delta \phi$, within the beat cycle at which the chirp occurs (Fig. 2). The time course of the AM (Fig. 2, *A–D*, *first* and *third* columns) is determined by the phase difference between the two EODs (Fig. 2, *A–D*, *middle* columns). During normal beats, the phase difference increases or decreases with constant slope. This slope is set by the difference frequency Δf_{Beat} between the EODf of the chirping and the EODf of the receiving fish. The absolute value of Δf_{Beat} is the frequency of the resulting beat AM. Throughout this article we calculate Δf as the frequency of the communicating fish, EODf₂, (i.e., the frequency of the stimulus) minus the frequency of the receiving fish, EODf₁. Thus Δf_{Beat} is positive if the stimulation frequency is above the EOD frequency of the recorded fish. A chirp always constitutes an increase in EODf₂. Therefore, the transient change in $\Delta f(t)$ that a chirp induces depends on both the value and the sign of the beat frequency Δf_{Beat} .

At positive Δf_{Beat} , when EODf₂ is greater than EODf₁, a chirp transiently increases $\Delta f(t)$ and thus briefly accelerates the beat AM (Fig. 1*D*). At low Δf_{Beat} , the chirp leads to a fast up- or downstroke depending on the phase of the beat at which it is emitted (Fig. 2*A*). At faster Δf_{Beat} , the chirp spans several periods of the beat and thus the beat phase at which it occurs is not as crucial anymore (Fig. 2*B*).

When EODf₂ is lower than EODf₁, Δf_{Beat} is negative and $\Delta \phi(t)$ decreases with time (Fig. 2, *C* and *D*, *middle* columns).

Now, the transient increase in EODf₂ caused by the chirp decreases $\Delta f(t)$ and thus slows down the beat. It could even invert the sign of $\Delta f(t)$. The latter occurs at Δf_{Beat} between -90 and 0 Hz and results in a plateau-like signal (Fig. 2*C*). At faster negative Δf_{Beat} , the chirp leads to a few periods of a slower beat (Fig. 2*D*).

Although the original communication signal, the chirp, is always the same (Fig. 2*E*), it causes a huge variety of AM signals depending on the underlying beat parameters (its frequency Δf_{Beat} and phase $\Delta \phi$). In the following we demonstrate how these different signals are encoded in the electrosensory system.

Chirps increase P-unit responses at slow positive difference frequencies. The AMs of both beats and chirps are encoded in P-unit electroreceptors. In the absence of a beat, the P-units fire randomly with a constant rate (Fig. 3, *A–D*, *left* columns). When the cell is stimulated with a slow beat (e.g., 10 Hz in Fig. 3, *A–D*, *middle* columns), its firing rate closely follows the stimulus. However, spike timing appears to exhibit a high degree of variability when compared across trials (Fig. 3*B*).

As was shown before (Benda et al. 2005, 2006), a small chirp increases the response of the cell when superimposed on such a slow beat. The peak of the firing rate during the chirp clearly exceeds that during the beat (Fig. 3*C*, *middle* column), although the maximal amplitude of the stimulus is the same during chirp and beat periods (Fig. 3*A*, *middle* column).

The shortest interspike interval of the response of the cell is determined by the frequency of the fish's EOD (Fig. 3*B*, *middle* column). During the fast upstroke of the chirp, the cell reaches this highest possible firing rate. Here, the interspike intervals are on the order of one EOD period, and consequently, the correlation over trials is high. The increase in firing rate is thus caused by both an increase in instantaneous firing rate as well as an increase in correlation across trials (Fig. 3*B*, *middle* column).

Chirps decrease P-unit responses at faster beats. At higher beat frequencies, for example, $\Delta f_{\text{Beat}} = 100$ Hz, the cell responds with an increased maximal firing rate of ~ 600 Hz to the beat (Fig. 3, *A–D*, *right* columns). Further, two action potentials are predominantly fired in response to each beat cycle (Fig. 3*B*, *right* column). In contrast to the slow beat described above, the chirp now decreases the peak firing rate (Fig. 3*C*) and the locking pattern breaks down during the chirp due to missing spikes (see spike raster in Fig. 3*B*).

Population activity is either synchronized or desynchronized by chirps. The receptor afferents are subject to uncorrelated noise whose source has not been identified but probably is channel noise (Chacron et al. 2005; Benda et al. 2006). This implies that the effects seen over subsequent trials recorded in single cells are expected to persist at the population level as well. To test this, we measured the population response in whole nerve recordings for the same chirp/beat combinations as used in single cell recordings. The population response is bigger the more afferents fire in synchrony and gets cancelled out as afferents fire asynchronously. A chirp on a slow beat increases the population activity (Fig. 3*D*, *middle* column), suggesting an increase in synchrony among cells. The population activity is already high in response to a faster beat (Fig. 3*D*, *right* column) and is decreased by the chirp. The population activity thus resembles the effects shown for the single cell and supports the assumption that the

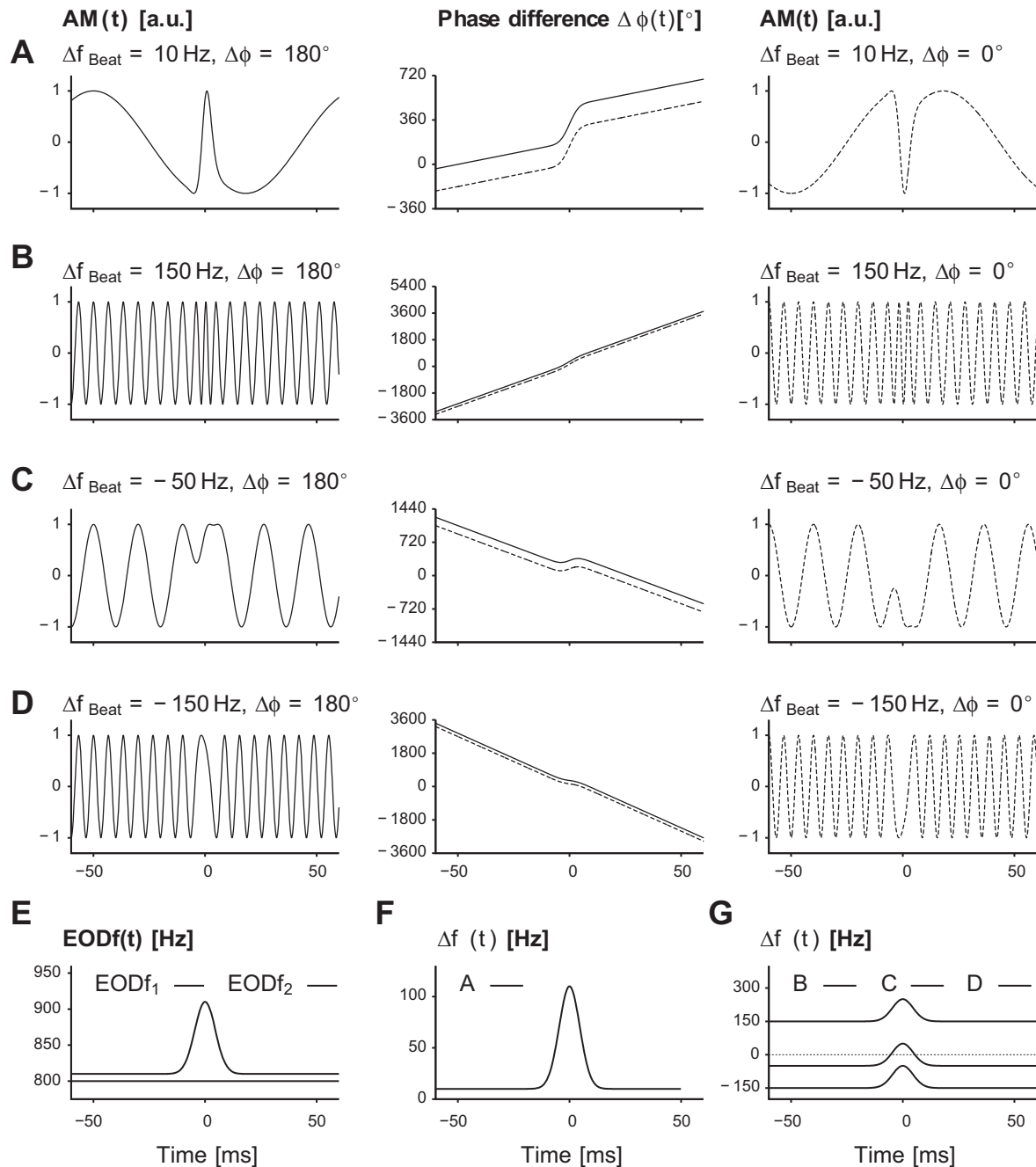


Fig. 2. Signals caused by chirps at different beats. *A–D*: characteristic AMs (*left and right columns*) are formed by the phase difference $\Delta\phi(t)$ between 2 EOD signals (*middle columns*). In all examples a chirp of width $\Delta t = 14$ ms and size $s = 100$ Hz was simulated centered around *time 0* (all values corresponding to Eq. 3). The stimulation frequency was chosen relative to the fish's EODf to form difference frequencies $\Delta f_{\text{Beat}} = 10, 150, -50,$ and -150 Hz as indicated. The *left columns* show the AM caused by a chirp occurring at beat phase $\Delta\phi_0 = 180^\circ$ (right in the trough of the beat), while the *right columns* show the same chirp at $\Delta\phi_0 = 0^\circ$ (at the peak of the beat). The phase differences (*middle columns*) are shown for both $\Delta\phi_0 = 180^\circ$ (solid line) and $\Delta\phi_0 = 0^\circ$ (dashed line). A phase difference of 360° corresponds to a single beat cycle. Note that the actual effects of a chirp on the AM also depend on its width and size. *E*: time course of the EOD frequency of a chirping fish with $\text{EODf}_2 = 810$ Hz (the "stimulus," dashed line) together with the EOD frequency of the receiving fish with $\text{EODf}_1 = 800$ Hz (solid line) for the same situation as shown in *A*; a.u., arbitrary units. *F*: chirp transiently changes the resulting time-dependent $\Delta f(t)$ from the background beat $\Delta f_{\text{Beat}} = \text{EODf}_2 - \text{EODf}_1 = 10$ Hz to maximally $\Delta f_{\text{Beat}} + s = 110$ Hz. This acceleration of the beat frequency mainly determines the resulting AMs (*left and right columns* in *A*). *G*: $\Delta f(t)$ for the beat frequencies shown in *B–D* as indicated. For a chirp on the slow negative $\Delta f_{\text{Beat}} = -50$ Hz from *C*, $\Delta f(t)$ crosses 0 Hz (dotted line) and reverses sign. On the fast negative $\Delta f_{\text{Beat}} = -150$ Hz from *D*, the frequency difference is transiently slowed down by the chirp.

correlation between trials recorded from single cells mirrors the synchrony among cells in a population.

Synchronization and desynchronization of P-unit activity at negative difference frequencies. The time course of a pure beat AM is determined only by the magnitude, not by the sign of the

difference frequency. At negative Δf_{Beat} that arise in interactions with an EOD of lower frequency than that of the receiving fish, the resulting beat AMs are thus the same as the AMs of the corresponding positive Δf_{Beat} . However, a chirp occurring on a beat of negative Δf_{Beat} causes quite different P-unit

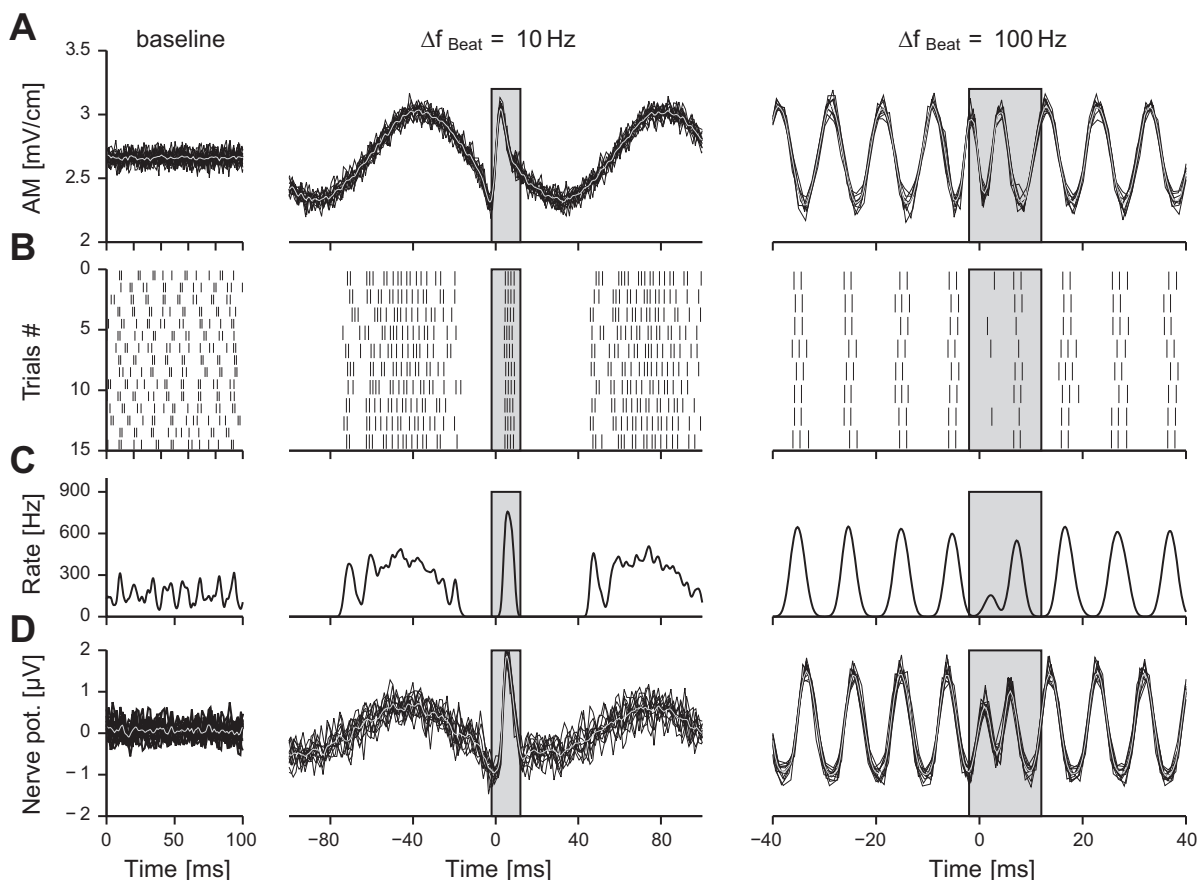


Fig. 3. Electroreceptor activity evoked by a chirp at positive difference frequencies. *A*: AM stimulus recorded at a site close to the fish's body under baseline conditions (no stimulus, *left column*), with a beat resulting from a difference frequency of $\Delta f_{\text{Beat}} = +10$ Hz (*middle column*), and with a beat of +100 Hz (*right column*). A chirp of size $s = 100$ Hz and width $\Delta t = 14$ ms was centered around *time 0*. Shown are individual AMs for each trial (black lines) and the average (gray line). *B*: spike raster of a single cell recording under the respective stimulus conditions. *C*: average firing rate computed by convolving the spike raster shown in *B* with a Gaussian kernel of 1-ms SD and averaging over trials. The timescale of the kernel resembles the fast component of the postsynaptic potential in the target cells (Berman and Maler 1998). *D*: population activity as recorded from the lateral line nerve with hook electrodes. Black lines depict results from single trials, and grey line is their average. The gray boxes mark the time window used for analyzing the responses to chirps.

responses compared with one occurring on the corresponding positive Δf_{Beat} . The chirp now decreases the absolute $\Delta f(t)$ (Fig. 2D).

At intermediate negative Δf_{Beat} , where the chirp transiently inverts the sign of the frequency difference and a plateau-like signal evolves (Fig. 2C), the response depends on where the plateau occurs, namely at which phase of the beat the chirp is emitted. In Fig. 4, *A–D*, *middle columns*, we show an example where the chirp occurs more towards the trough in the beat, and the cells cease firing. They keep on firing at high levels if the chirp occurs at the peak of the beat (not shown). For all cases, the correlation between trials decreases in response to this slow signal. At very fast beats, where the response to beats is reduced due to the high frequency, it is now transiently increased by the chirp (Fig. 4, *A–D*, *right columns*).

Four distinct regimes for encoding chirps at different beat frequencies. The examples shown so far suggest a strong influence of Δf_{Beat} on the synchronization or desynchronization of the P-unit response by a chirp. In the following we will systematically examine this effect and quantify the P-unit responses by the CSI, i.e., the contrast between the responses to chirps and beats (see MATERIALS AND METHODS and Vonderschen and Chacron 2011). As the response of P-units fluctuates around a mean firing rate, we determined the CSI in terms of

the firing rate fluctuation (as calculated by the standard deviation) and the correlation over trials.

The CSIs pooled over all single unit recordings ($n = 220$ cells) as well as over all ($n = 9$) population recordings confirm the impression of the example recordings shown above (note that we included repeated measurements of 3 of the 6 nerves from which we had performed whole nerve recordings). There are four regimes of Δf_{Beat} in which the firing rate, the spike correlation, and the population activity are affected in the same way by a chirp of size $s = 100$ Hz (Fig. 5, *A–C*, *left columns*): at large negative Δf_{Beat} (below -100 Hz), the CSI is greater than zero, indicating an increase in firing rate as well as synchrony in response to the chirp (*regime 1* in Fig. 5). At slow negative Δf_{Beat} between -80 and -20 Hz, the chirp desynchronizes the P-unit responses ($\text{CSI} < 0$; *regime 2*). For positive Δf_{Beat} , the opposite happens: at low beat frequencies between about 0 and 30 Hz, the CSI is positive again (synchronization, *regime 3*), while all beats faster than 30 Hz lead to a CSI less than zero (desynchronization, *regime 4*). At these high beat frequencies, the effect is less prominent for spike correlations. The results at most Δf_{Beat} differ statistically significantly from zero [$P < 0.05$ and corrected with a modified Bonferroni correction, Simes method (Simes 1986)], indicating that chirps affect the responses and that both effects, decreases

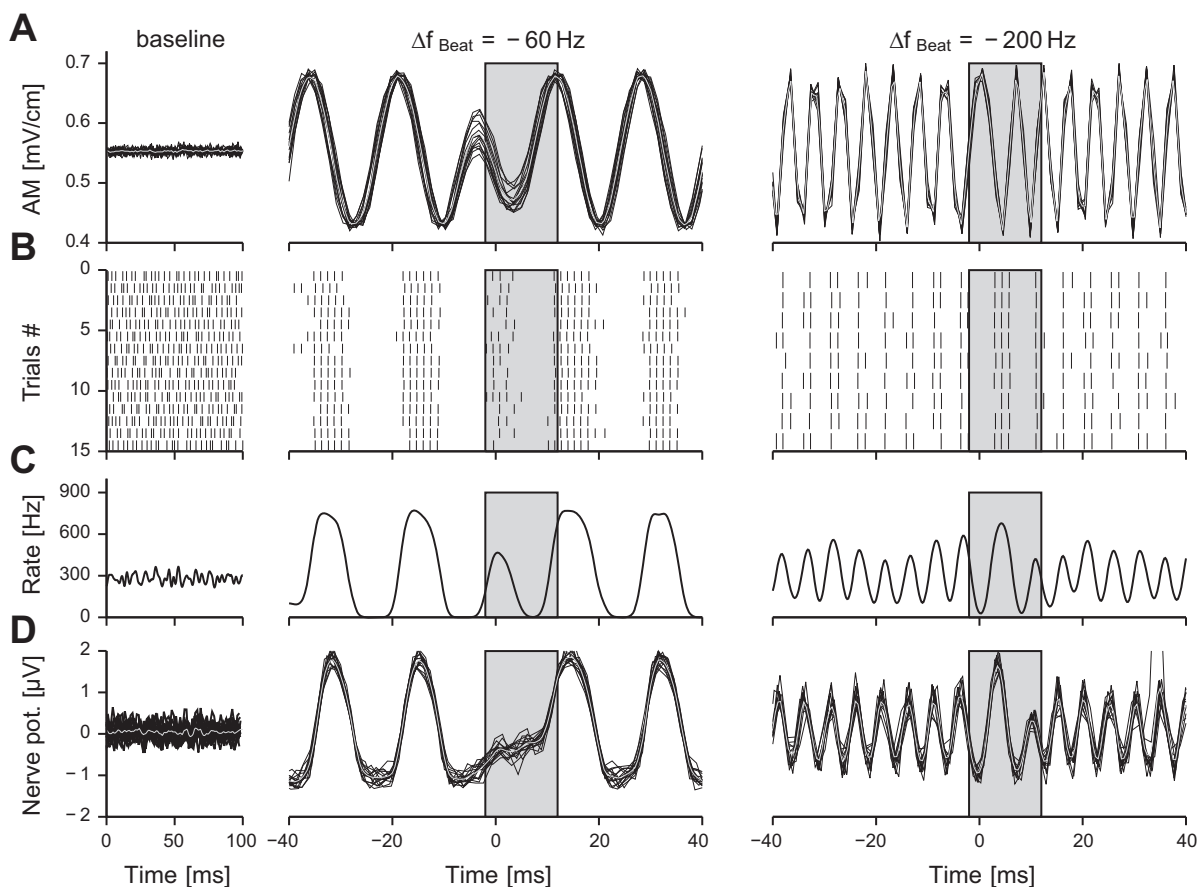


Fig. 4. Electrophysiological activity evoked by a chirp at negative difference frequencies. *A–D*: same as in Fig. 3 for beats resulting from difference frequencies of $\Delta f_{\text{Beat}} = -60$ Hz (middle columns) and -200 Hz (right columns). Note, that the shown data originate from a different subject than that in Fig. 3 and, therefore, exhibit a different baseline activity.

as well as increases in the response, are consistent and reliable over cells. Values at the zero-crossings, where the CSI changes from being positive to being negative or vice versa, are not distinguishable from zero.

Similar results are obtained for the responses to chirps with a smaller size of 60 Hz (Fig. 5, *A–C*, right columns). However, effects are smaller at many Δf_{Beat} , especially at high positive ones (arrow 1 in Fig. 5*B*, right column). Accordingly, many values are not significantly different from zero (significance is indicated by asterisks), particularly regarding correlation across trials. Also, the zero crossings of the CSI curves slightly differ between the 100-Hz chirp and the 60-Hz chirp (arrows 2 and 3 in Fig. 5*B*).

In summary, chirps are encoded by P-units over the whole behaviorally relevant repertoire of beats. However, depending on Δf_{Beat} , a chirp either synchronizes or desynchronizes the P-unit population, leading to either an increase or decrease of both the response rate and correlation across trials. This partitions the Δf_{Beat} in four distinct regions. In the following we analyze how the responses to chirps are generated and how cell heterogeneity and more detailed aspects of a chirp influence the response to chirps.

Predicting the response to chirps from frequency tuning. As described above, a chirp increases the frequency difference $\Delta f(t)$ for a short time (Fig. 2) and with that transiently modulates the frequency of the resulting AM that is encoded by the P-units. The response of a P-unit to a chirp could therefore be

predictable solely from its tuning to sinusoidal AMs of different frequencies, i.e., beats. The single cell responses to sinusoidal AM stimuli show a peak in modulation depth of the firing rate as well as in correlation at intermediate AM frequencies between 50 and 80 Hz and a decrease for slower and faster frequencies (Fig. 6, *A* and *B*). Their response to beats of negative Δf_{Beat} is the same as for those of positive Δf_{Beat} . This is expected as the beat AM of a certain positive Δf_{Beat} is the same as that of the corresponding negative Δf_{Beat} .

The tuning of the population response closely matches the tuning of spike-train correlations measured in single cells (compare Fig. 6, *B* and *C*). The largest modulation of the population response and thus the highest synchronicity are found at the same intermediate beat frequencies. Note that all three tuning curves are symmetrical around zero, because the AM of a beat of negative Δf_{Beat} is the same as that for a positive one.

To predict the response to a chirp with a size of $s = 100$ Hz, we read off the response from the AM frequency tuning curves obtained from the whole nerve recordings at 60 Hz (approximately the average change in frequency evoked by this chirp) to the right of Δf_{Beat} (Fig. 7*A*). For most Δf_{Beat} , these predictions of the response to the chirp match the measured data well (Fig. 7*B*), indicating that the cells mainly respond to the change in $\Delta f(t)$ induced by the chirp. The response to chirp-induced frequency changes is rapid since the prediction also works for

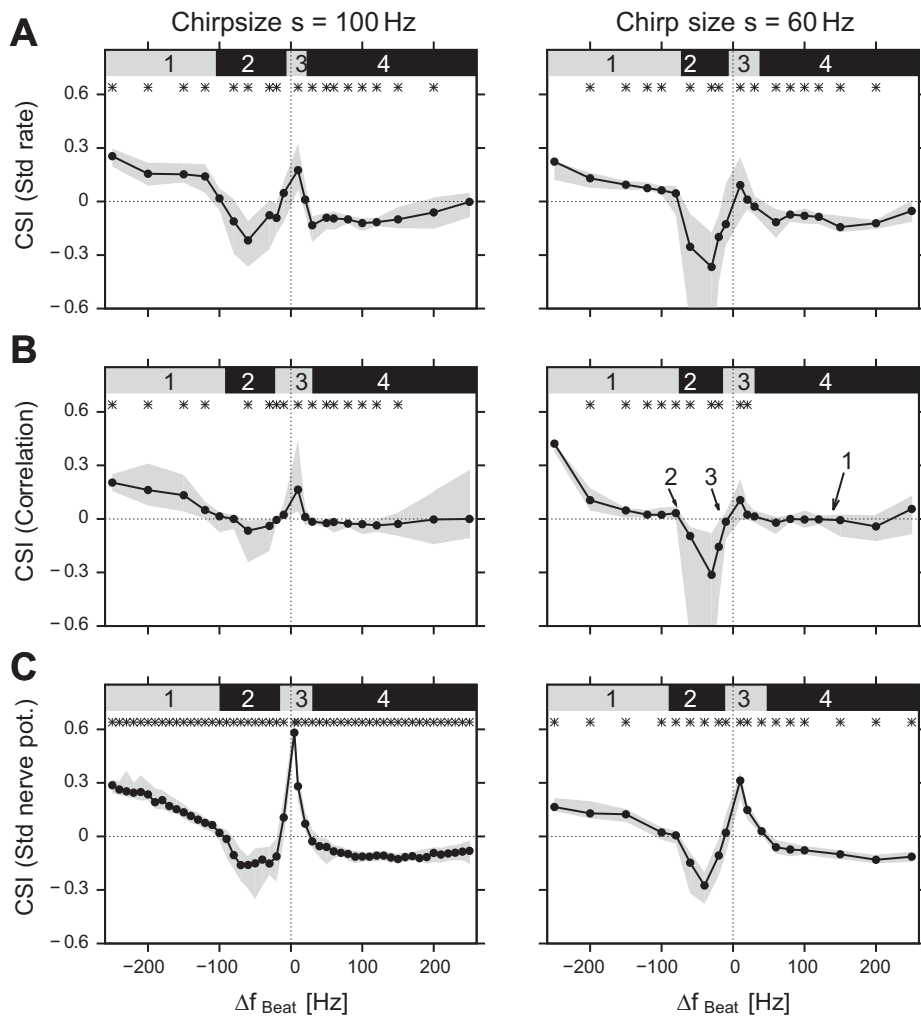


Fig. 5. Representation of chirps in electroreceptor activity depends on difference frequency. The chirp selectivity index (CSI) measures the contrast between the response to the chirp and the response to the beat. *A*: average firing rate computed in a window around the chirp (gray boxes in Figs. 3 and 4) and during the beat is used as a measure for the single unit response. Shown are the median (solid line) and the interquartile range (shaded area) of all CSI values pooled over beat phases, contrasts, and cells. *B*: CSI of single units based on spike correlation across trials. The arrows point to differences between the *left* and *right* columns that are referred to in the text. *C*: CSI obtained from the population activity as the SD of the potential recorded from the lateral line nerve. Gray and black bars indicate beat frequencies where chirps have synchronizing (CSI > 0) or desynchronizing (CSI < 0) effects, respectively. The different regimes are numbered from 1 to 4. Difference from zero was assessed by a sign test (Bonferroni corrected) in all cases, and those values significantly different from zero ($*P > 0.05$) are indicated. *Left* columns show the responses to a chirp of size $s = 100$ Hz and in the *right* columns to one of size $s = 60$ Hz.

low beat frequencies where the higher Δf during the chirp results in less than a full beat cycle.

With this procedure we then computed the CSI for every beat frequency (Fig. 7C). Small differences between predicted and measured CSI are seen for fast positive Δf_{Beat} (> 120 Hz) where the measured desynchronization is weaker than predicted and for intermediate negative beats ($\Delta f_{\text{Beat}} \approx 30$ Hz), where higher CSI values are predicted. The latter is the region in which the phase relation between chirp and beat influences the response. The phase is not considered in the prediction, and deviations are therefore not surprising.

The prediction based on AM frequency tuning was robust with respect to the particular value used for shifting the tuning curve during the chirp (Fig. 7C, *inset*). Also, computing a more precise prediction by considering the chirp's shape did not improve the prediction (not shown).

Sources of single cell response variability. The estimates of the CSI derived from single unit responses (Fig. 5, *A* and *B*) show a considerable amount of variability when pooled over cells and animals. In contrast, the CSIs computed from the population rates are much more reliable, since the variability between single cells is already averaged out in the measurement (Fig. 5C). In both cases, we pooled all data irrespective of the phase at which the chirps occurred within a beat cycle. Chirps at different phases $\Delta\phi_0$ of the beat give rise to very

different AMs (Fig. 2; see also Walz et al. 2013; Zupanc and Maler 1993) and thus to potentially different responses of the P-units (see below). To disentangle the influence of cell heterogeneity and phase, we averaged over each factor separately and analyzed the remaining variability.

When averaging the responses over beat phases first, the remaining variability is caused by cell heterogeneity (Fig. 8A) and appears to be large. The variability caused by different phases of the chirp within the beat (Fig. 8B) is markedly lower except for intermediate negative beat frequencies. Comparing the standard deviation of CSI estimates when averaged over cells or over beat phases indicates that indeed the variability over cells is greater than that over phases (Fig. 8C). The responses of single cells are apparently more strongly affected by their heterogeneous properties than by the difference in stimulus shape caused by different beat phases where the chirp occurs.

Discrimination of different chirps. We next asked whether an upstream neuron could in principle distinguish chirps occurring at different phases $\Delta\phi_0$ of the beat. Especially at slow beats the particular phase at which a chirp occurs in a beat cycle has a strong impact on the resulting AM (Fig. 2). This appears to be reflected in the spike responses (Fig. 9A).

For analyzing the differences between spike trains evoked by chirps at different $\Delta\phi_0$, we performed a discrimination

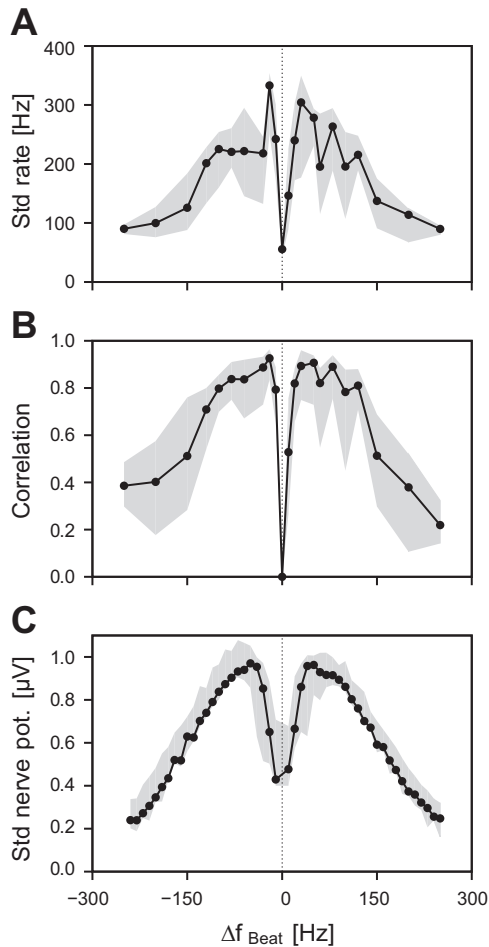


Fig. 6. AM frequency tuning of P units. The responses to the pure beat stimulus as a function of difference frequency Δf_{Beat} (based on the same responses as in Fig. 5). The responses are averages of the SD of the single cell firing rate as a measure for the rate modulation depth (A), the correlation between pairs of spike-trains as a measure of synchrony (B), and the population activity computed as the SD of the voltage recorded from the lateral line nerve in a window during the beat (C). Shown are median (solid line) and interquartile range (gray).

analysis similar to Marsat and Maler (2010) and Vonderschen and Chacron (2011) on the basis of spike distance metrics (van Rossum 2001). To determine whether the responses to different $\Delta\phi_0$ were clearly distinguishable, we constructed confusion matrices over 10 different bins of beat phases indexed by a (Fig. 9B) by assigning each single spike train to the bin b of beat phases that elicited the spike trains it was most similar to. Perfect distinction would lead to matrices that have nonzero values only on the diagonal. The confusion matrices were constructed for each Δf_{Beat} and time scale τ_c of the distance measure Eq. 6 and each cell and subsequently averaged over cells. How well spike trains evoked by chirps on different beat phases can be assigned correctly is quantified by the relative mutual information I_{rel} of the confusion matrix in Eq. 8. For each Δf_{Beat} and each temporal resolution tested, a single value is obtained that is color coded in Fig. 9, C and D (see MATERIALS AND METHODS). A high information in the confusion matrix, corresponding to a light color in Fig. 9, C and D, reflects a good discriminability of the responses evoked by chirps at different beat phases.

Generally, the responses to chirps occurring at different phases of the beat can be well discriminated at slow beats while discrimination becomes more difficult at higher beat frequencies (darker colors in Fig. 9, C and D). Discrimination performance is markedly improved at higher beat frequencies when

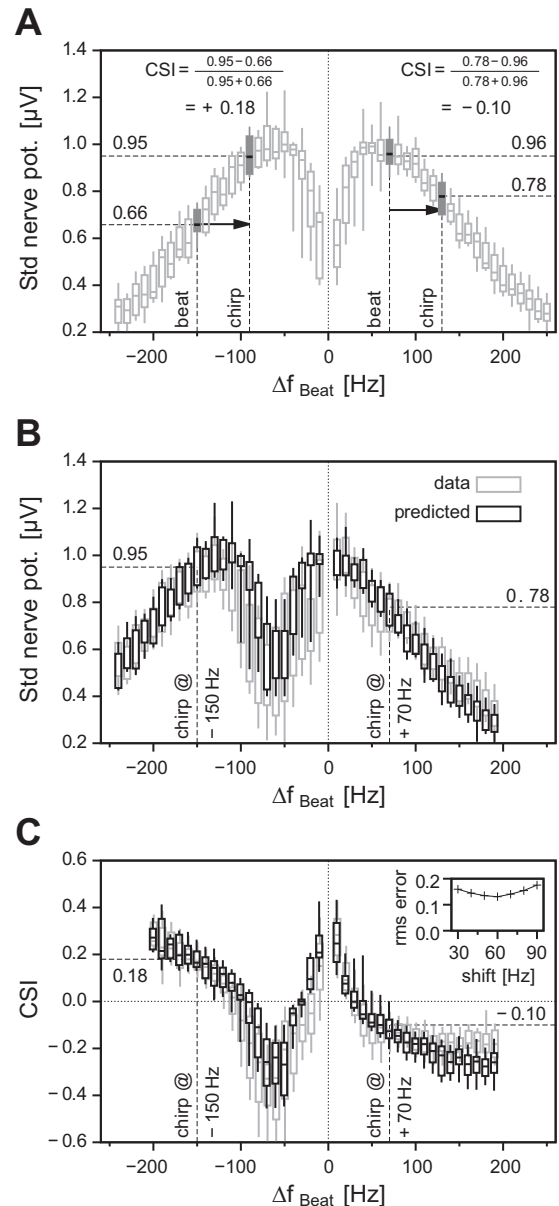


Fig. 7. Predicting the response to a chirp solely from the AM frequency tuning. A: prediction procedure. The average frequency excursion of a chirp with a maximum of 100 Hz over 14 ms is ~ 60 Hz. We predicted the response to the chirp from the response to a beat with a frequency shifted by this 60 Hz to the right with respect to the underlying beat. For example, the response to a chirp on top of a beat of $\Delta f_{\text{Beat}} = -150$ Hz was predicted to be the same as a response to a pure beat of $\Delta f_{\text{Beat}} = -150$ Hz + 60 Hz = -90 Hz. At a beat of $\Delta f_{\text{Beat}} = 70$ Hz, the prediction was read off as the response to a beat of $\Delta f_{\text{Beat}} = 70$ Hz + 60 Hz = 130 Hz, as demonstrated. The same applies to all other Δf_{Beat} . With the predicted response, the CSI can be calculated as for the measured data. The predictions were done on the data from individual nerves and then averaged over nerves. Note that the procedure is demonstrated here on median values to simplify the illustration. B: predicted nerve response during the chirps is shown together with the measured ones as a function of Δf_{Beat} . C: predicted CSI compared with the measured CSI. Inset: root mean squared error of the prediction for different shift values used for approximating the effect of the chirp.

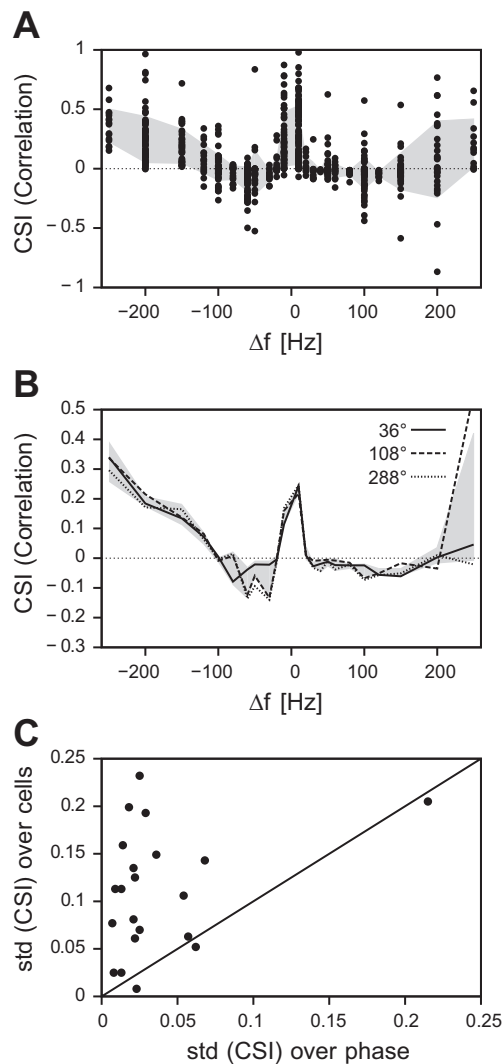


Fig. 8. Sources of variability. *A*: CSI (based on the correlation over trials) computed from responses to chirps of $s = 100$ Hz in dependence on beat frequencies (same data as in Fig. 5). *B*: here the CSI is averaged over all phases $\Delta\phi$ for each cell separately (each black circle is the average of a single cell). Gray area represents means \pm SD of the CSI estimates. *B*: same data as in *A*, but now averaged over cells for 10 classes of beat phases $\Delta\phi$, i.e., the time of occurrence of a chirp within a beat cycle. Three phase classes are drawn as indicated; the gray area marks the means \pm SD of the 10 phase classes as a function of beat frequency. *C*: comparison of CSI variability when averaging over cells or phase. For each underlying beat frequency Δf_{Beat} , the SD of the CSI estimations when averaged over cells (gray area in *A*) is plotted over the SD of the estimation when averaged over cells (gray area in *B*). Points lying above the diagonal exhibit a greater variability resulting from cell heterogeneity than from different phases of chirp stimulation.

temporal resolution of the distance measure is fine ($\tau_c = 1$ ms, Eq. 6). On the contrary, at slow beats good discrimination can be achieved with a wide range of temporal resolutions. This matches the natural time scales of the AM waveforms induced by the chirps. However, for all beat frequencies up to 100 Hz, the discrimination is possible at the physiologically relevant time scale on the order of milliseconds.

Increasing the width of the analysis interval simply increases discrimination performance since more information becomes available for the discrimination. The dependence on Δf_{Beat} and temporal resolution is, however, not influenced by the width of the analysis interval (compare *left* and *right* columns in Fig. 9,

C and *D*). The size s of the chirp, i.e., its maximal frequency excursion, also influences discrimination performance. Discrimination is elevated for the 100-Hz chirp compared with the 60-Hz chirp (compare Fig. 9, *D* and *C*, respectively).

DISCUSSION

Our data demonstrate that the very same stereotyped communication signal, the small chirp of the weakly electric fish *A. leptorhynchus*, is encoded in two opposing ways. Depending on the frequency of the ongoing background signal, the beat, the chirp transiently either synchronizes or desynchronizes the activity of the receptor population. In fact, the range of naturally occurring beat frequencies is partitioned into four regimes where synchronization alternates with desynchronization. In contrast to a previous study where synchronization was attributed to small chirps and desynchronization to a different type of chirps (large chirps, Benda et al. 2006), we focused here on the neural responses elicited by a single type of chirp occurring in different social contexts that are reflected by the frequency of the background beat. Since male EODf are typically higher than female ones (Meyer et al. 1987; Zakon and Dunlap 1999) and larger fish carry higher frequencies than smaller fish (Triefenbach and Zakon 2008; Fugère et al. 2011), low-beat frequencies result from same-sex, aggressive and high ones from opposite-sex, submissive encounters. We chose the small chirp as it is the most commonly emitted signal in most contexts (Zupanc 2002) and used background frequencies that fish are likely to encounter in the wild (Stamper et al. 2010).

Critical to a perception of signals is their representation at higher brain areas. Does the differential encoding of small chirps at different background frequencies persist at such subsequent processing stages and thus correspond to a differential perception? P-units project with distinct convergence ratios onto pyramidal cells in three different maps of the ELL (Heiligenberg and Dye 1982; Carr et al. 1982; Maler 2009). As shown by lesion experiments, the lateral segment (LS) of the ELL is necessary for chirping behavior (Metzner and Juranek 1997). In this map, $\sim 1,000$ electroreceptor afferents converge onto each pyramidal cell (Maler 2009). The resulting large receptive fields together with a readout based on coincidence detection explain their high-pass response properties (Krahe et al. 2008; Middleton et al. 2009). The pyramidal cells of the LS should therefore be sensitive to changes in the level of synchrony of the P-unit population as measured here by spike train correlations and whole nerve recordings. Indeed, LS pyramidal cells of the E-type encode small chirps on low difference frequencies in synchronized bursts, whereas large chirps on high difference frequencies, which desynchronize P-units (Benda et al. 2006), are encoded by I-cells (Marsat et al. 2009). We expect that depending on the beat small chirps are encoded by E-cells whenever they synchronize the P-unit population and by I-cells in case they desynchronize the P-units. Thus small chirps would be encoded in two different processing streams depending on the background difference frequency.

The result of four encoding regimes is largely independent of the assumed readout of the P-unit population, as the firing rate as well as correlations between spike trains give similar results. This similarity is not surprising since P-units are independent (Benda et al. 2006; Chacron et al. 2005) and their mean firing rate is the same during beats and chirps (Benda et

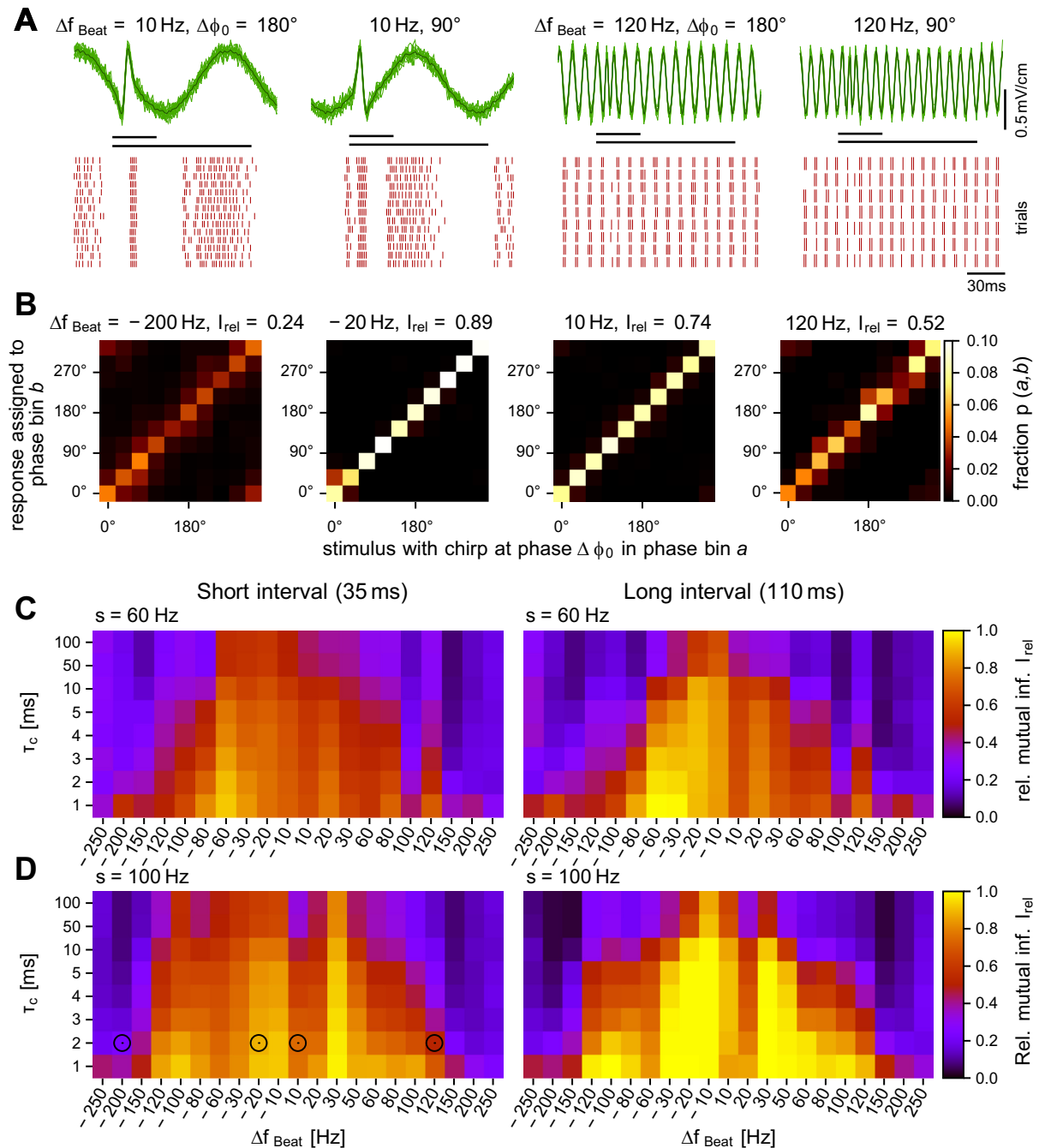


Fig. 9. Discriminability of chirp responses at different beat phases. *A, top*: AMs of 2 different beats ($\Delta f_{\text{Beat}} = 10$ and 120 Hz) superimposed with chirps occurring at different phases of the beat ($\Delta\phi = 180$ and 90°). Black bars indicate the 2 intervals used for the discrimination analysis (short interval spanning the chirp only and long interval also including parts of the beat). *A, bottom*: rasterplots of the corresponding neuronal responses. *B*: confusion matrices created from assigning each spike train evoked by a chirp occurring at the beat phase $\Delta\phi_0$ in bin *a* to the phase bin *b* that had elicited a set of spike trains; this spike train had the smallest distance to as estimated by Eq. 6. The confusion matrices were then averaged over cells, and their relative mutual information was calculated (Eq. 8). Subplots show confusion matrices for different beat frequencies Δf_{Beat} as indicated and a chirp size of 100 Hz using the time-constant $\tau_c = 2 \text{ ms}$ and the short analysis window for estimating the distance between spike trains. *C*: discrimination performance (in terms of the relative mutual information) of a chirp of size $s = 60 \text{ Hz}$ as a function of Δf_{Beat} and the temporal resolution τ_c of the distance measure (Eq. 6) for the short (*left plot*) and long (*right plot*) analysis intervals. *D*: same as *C* but for responses to a chirp of size $s = 100 \text{ Hz}$. Circles at *left* mark the corresponding confusion matrices shown in *B*.

al. 2006). In the centrolateral and the centromedial segments (CLS and CMS) of the ELL, neither E-cells nor I-cells show such strong responses to chirps as in the LS (Marsat et al. 2009). In these segments, receptive field sizes are smaller. About 150 (CLS) or 40 (CMS) P-unit afferents project onto each pyramidal cell (Maler 2009). This makes an additive

readout of P-unit activity as quantified by the firing rate more likely.

Our results focus on the responses evoked by chirps directly. However, a chirp also induces a phase shift of the beat (Fig. 1D; Benda et al. 2005). Superficial E-cells that encode small chirps on slow beats (Marsat et al. 2009) receive indirect

feedback (Berman and Maler 1998) that predicts and cancels responses to low-frequency ongoing beats (Bastian et al. 2004). After a chirp the beat and the feedback are out of phase, resulting in an enhanced response (Marsat and Maler 2012). The cancellation of beat responses by the feedback only works up to AM frequencies of 20 Hz and is thus unlikely to enhance chirp responses at higher difference frequencies. Thus, at AM frequencies larger than 20 Hz that occur mostly during social encounters (Stamper et al. 2010), chirp-induced phase shifts of the beat are not processed by the indirect feedback of the ELL.

The AM waveform a chirp induces not only depends on its size, duration, and the difference frequency, but also on the phase at which the chirp occurs during the beat (Fig. 2). Indeed, responses to the same chirp at different beat phases can be well discriminated at low difference frequencies (Fig. 9). This is preserved in ELL pyramidal cells as well as in dense coding cells of the torus semicircularis (Vonderschen and Chacron 2011). The large differences in AM waveforms and the corresponding neural responses caused by different beat phases were demonstrated to hinder discrimination of chirps of different sizes and durations in pyramidal cell responses (Marsat and Maler 2010). However, at difference frequencies larger than ~ 100 Hz, P-unit responses to chirps of a particular size and width become more and more similar independent of their phase in the beat (Fig. 9), thus potentially allowing to discriminate properties of different types of chirps. This behaviorally relevant range of difference frequencies (Stamper et al. 2010) was not tested in the mentioned ELL studies. Discrimination of chirps in P units performed best at time constants of 1 ms in contrast to ~ 5 ms in pyramidal cells (Marsat and Maler 2010; Vonderschen and Chacron 2011), following the general pattern of less precise spike responses in upstream neurons both in vertebrates (Kara et al. 2000) and invertebrates (Vogel et al. 2005). For future analysis of chirp discrimination in P-units, population responses have to be taken into account, since variability between different cells is even larger than between responses of a single cell to chirps at different beat phases (Fig. 8).

Because the rate of emitted small chirps strongly decreases with larger difference frequencies (Engler and Zupanc 2001; Bastian et al. 2001) and recordings of P-unit responses suggested vanishing responses at beat frequencies beyond 60 Hz (Benda et al. 2005), all electrophysiological studies on chirp encoding considered difference frequencies only up to this frequency (Benda et al. 2006; Marsat et al. 2009; Marsat and Maler 2010; Vonderschen and Chacron 2011). However, large difference frequencies up to 300 Hz do occur naturally (Stamper et al. 2010) and chirps at larger difference frequencies do have significant effects on echo responses and attack behavior (Hupé and Lewis 2008; Hupé et al. 2008). Our data on P-unit responses to chirps demonstrate that chirps are indeed encoded by P-units in the full range of possible positive and negative difference frequencies.

Surprisingly, chirps as transient and stereotyped communication signals (Zakon et al. 2002; Hupé and Lewis 2008) turned out not to be encoded by P-units irrespective of context parameters like the difference frequency. Rather the space of difference frequencies is divided into four regimes where synchronizing chirp responses alternate with desynchronizing responses (Fig. 5). Since difference frequency carries important information about social context in terms of gender (Meyer et al. 1987; Zakon and Dunlap 1999), size (Zakon and Dunlap

1999; Dunlap 2002), and dominance (Dunlap 2002; Triefenbach and Zakon 2008; Fugère et al. 2011), our findings suggest two opposing hypotheses. Either small chirps have the same meaning at all difference frequencies and then one would expect to find neurons further upstream that respond in the same way to small chirps irrespective of difference frequency or different behavioral categories of chirps exist that reflect the categorical representation that we find on the receptor level.

Following the second hypothesis we suggest that small chirps at large difference frequencies could be used by the fish to determine the sign of the difference frequency. How fish sense the sign of the difference frequency has been studied in detail in *Eigenmannia* in the context of the jamming avoidance response for low difference frequencies (Bullock and Heiligenberg 1986; Kawasaki et al. 1988). However, at high difference frequencies, this mechanism, which is based on a comparison between amplitude and phase modulation signals evoked by the beat, has not been studied yet. Because the phase modulation induced by the beat results in smaller and smaller time shifts that have to be detected by the T-unit system (Heiligenberg and Partridge 1981) as the beat frequency increases, this mechanism might not work at high beat frequencies. Alternatively, since small chirps either synchronize or desynchronize the P-unit population at large negative or positive difference frequencies, respectively, chirping could provide the necessary cue whether the fish's frequency is higher or lower than that of its opponent.

Our study on the encoding of a communication signal was triggered by behavioral observations demonstrating the utilization of this signal on a much broader context than previously assumed (Hupé et al. 2008). The results showed a much richer response diversity on this broader space of natural stimuli. Like many recent unexpected findings from the visual system of vertebrates (e.g., Vinje and Gallant 2000; Butts et al. 2007) and invertebrates (van Hateren et al. 2005) as well as in the auditory system (Nelken et al. 1999; Theunissen et al. 2000), this emphasizes the importance of natural stimuli when studying neural function. In turn, our results on the context-dependent encoding of one type of chirps by electroreceptors call for more detailed behavioral as well as electrophysiological studies that take into account the full range of natural and behaviorally relevant stimuli.

The dependence of P-unit activity on frequency differences can be explained by a simple model based on the static AM frequency tuning curve of the neuron. As demonstrated in Fig. 7, the synchronization behavior of the P-units in response to the chirps is mainly based on their AM frequency tuning. A chirp transiently increases the frequency difference and thus modulates the AM frequency. The neuronal response rapidly follows this shift of AM frequency according to the AM frequency tuning curve. The good performance of the model highlights how fast the P-units respond to changes in stimulus frequency. As the chirp width is only 14 ms and thus shorter than one period of many of our beat stimuli, P-units already respond to fractions of a beat cycle (see, for example Fig. 3, *A–D, middle columns*). Because P-unit action potentials lock onto the EOD (Hagiwara and Morita 1963), their membrane time constant is likely to be shorter than a single EOD period (~ 1 ms) and thus potentially explains the ability of the P-units to quickly follow such a mean-coded signal. Cortical neurons also have been shown to rapidly follow mean-coded signals

(Boucein et al. 2009; Tchumatchenko et al. 2011). A variance-coded transmission that was suggested for rapid signal transmission (Silberberg et al. 2004) is therefore not required.

The AM frequency tuning curves for both rate modulation and correlations as the basis for predicting chirp responses show a band-pass tuning with maximal values in the range of 30–80 Hz (Fig. 6). Such a band-pass frequency tuning is found in neurons of various sensory systems (auditory: Narayan et al. 1998; vestibular: Straka et al. 2005; visual: Saul and Humphrey 1990) and is thus not a specific characteristic of P units. The high-pass component of the tuning curve of the P units (Nelson et al. 1997) has been attributed to rapid spike-frequency adaptation (Benda et al. 2005). Note that adaptation currents in general attenuate responses to low-frequency components of the stimulus thereby shaping a high-pass filter (Benda and Herz 2003). The low-pass component could simply originate from the firing rate of the P units (Knight 1972; Pressley and Troyer 2011) that have a high baseline activity of about 100–250 Hz (Gussin et al. 2007). The AM frequency tuning is static with respect to the time scales of AMs induced by beats and chirps considered here. The tuning may, however, change on longer time scales.

In addition to these basic mechanisms of the spike generator, the receptor current itself could already be band-pass tuned. While this is not the case for P units, since the tuning we consider here is with respect to the AM of a carrier signal, auditory nerve fibers, for example, are band-pass tuned by the cochlear filter to their characteristic sound frequency (Narayan et al. 1998). Many behaviorally relevant signals in acoustic communication as well as echolocation involve frequency shifts like the chirps in electrocommunication discussed here (see, e.g., Bailey et al. 1993; Wang et al. 1995). The study of their encoding has been focused on more complex aspects such as the selectivity for spectro-temporal features (Zhang et al. 2003). However, the fast and robust encoding of transient signals in peripheral receptors could also be based on the simple frequency-tuning mechanism described above. This mechanism does not require unique properties in receptor cells and could therefore be a universal mechanism for fast encoding of transient periodic signals.

ACKNOWLEDGMENTS

We thank Franziska Kümpfbeck for conducting some of the P-unit recordings and Rüdiger Krahe for helpful discussions.

GRANTS

This work was supported by the BMBF Bernstein Award Computational Neuroscience Grant 01GQ0802 (to J. Benda).

DISCLOSURES

No conflicts of interest, financial or otherwise, are declared by the author(s).

AUTHOR CONTRIBUTIONS

Author contributions: H.W., J.G., and J.B. conception and design of research; H.W. and J.G. performed experiments; H.W. analyzed data; H.W., J.G., and J.B. interpreted results of experiments; H.W. prepared figures; H.W. drafted manuscript; H.W., J.G., and J.B. edited and revised manuscript; H.W., J.G., and J.B. approved final version of manuscript.

REFERENCES

- Bailey W, Greenfield M, Shelly T. Transmission and perception of acoustic signals in the desert clicker, *Ligurotettix coquilletti* (orthoptera: Acrididae). *J Insect Behav* 6: 141–154, 1993.
- Bastian J, Chacron MJ, Maler L. Plastic and nonplastic pyramidal cells perform unique roles in a network capable of adaptive redundancy reduction. *Neuron* 41: 767–779, 2004.
- Bastian J, Schniederjan S, Nguyenkim J. Arginine vasotocin modulates a sexually dimorphic communication behavior in the weakly electric fish *Apteronotus leptorhynchus*. *J Exp Biol* 204: 1909–1923, 2001.
- Benda J, Herz AV. A universal model for spike-frequency adaptation. *Neural Comput* 15: 2523–2564, 2003.
- Benda J, Longtin A, Maler L. Spike-frequency adaptation separates transient communication signals from background oscillations. *J Neurosci* 25: 2312–2321, 2005.
- Benda J, Longtin A, Maler L. A synchronization-desynchronization code for natural communication signals. *Neuron* 52: 347–358, 2006.
- Berman NJ, Maler L. Inhibition evoked from primary afferents in the electrosensory lateral line lobe of the weakly electric fish (*Apteronotus leptorhynchus*). *J Neurophysiol* 80: 3173–3196, 1998.
- Boucein C, Tetzlaff T, Meier R, Aertsen A, Naundorf B. Dynamical response properties of neocortical neuron ensembles: multiplicative versus additive noise. *J Neurosci* 29: 1006–1010, 2009.
- Bullock TH, Heiligenberg W (Editors). *Electroreception*. New York: John Wiley & Sons, 1986.
- Butts DA, Weng C, Jin J, Yeh CI, Lesica NA, Alonso JM, Stanley GB. Temporal precision in the neural code and the timescales of natural vision. *Nature* 449: 92–95, 2007.
- Carr CE, Maler L, Sas E. Peripheral organization and central projections of the electrosensory nerves in gymnotiform fish. *J Comp Neurol* 211: 139–153, 1982.
- Chacron MJ, Maler L, Bastian J. Electrorceptor neuron dynamics shape information transmission. *Nat Neurosci* 8: 673–678, 2005.
- Cherry EC. Some experiments on the recognition of speech, with one and with two ears. *J Acoust Soc Am* 25: 975–979, 1953.
- Dunlap KD. Hormonal and body size correlates of electrocommunication behavior during dyadic interactions in a weakly electric fish, *Apteronotus leptorhynchus*. *Horm Behav* 41: 187–194, 2002.
- Dye J. Dynamics and stimulus-dependence of pacemaker control during behavioral modulations in the weakly electric fish, *Apteronotus*. *J Comp Physiol A* 161: 175–185, 1987.
- Engler G, Fogarty CM, Banks JR, Zupanc GK. Spontaneous modulations of the electric organ discharge in the weakly electric fish, *Apteronotus leptorhynchus*: a biophysical and behavioral analysis. *J Comp Physiol A* 186: 645–660, 2000.
- Engler G, Zupanc GK. Differential production of chirping behavior evoked by electrical stimulation of the weakly electric fish, *Apteronotus leptorhynchus*. *J Comp Physiol A* 187: 747–756, 2001.
- Fugère V, Ortega H, Krahe R. Electrical signalling of dominance in a wild population of electric fish. *Biol Lett* 7: 197–200, 2011.
- Gifford GW, MacLean KA, Hauser MD, Cohen YE. The neurophysiology of functionally meaningful categories: macaque ventrolateral prefrontal cortex plays a critical role in spontaneous categorization of species-specific vocalizations. *J Cogn Neurosci* 17: 1471–1482, 2005.
- Gussin D, Benda J, Maler L. Limits of linear rate coding of dynamic stimuli by electroreceptor afferents. *J Neurophysiol* 97: 2917–2929, 2007.
- Hagedorn M, Heiligenberg W. Court and spark: electric signals in the courtship and mating of gymnotoid fish. *Anim Behav* 33: 254–265, 1985.
- Hagiwara S, Morita H. Coding mechanisms of electro-receptor fibers in some electric fish. *J Neurophysiol* 26: 551–567, 1963.
- Heiligenberg W, Dye J. Labeling of electroreceptive afferents in a gymnotoid fish by intracellular injection of hrp: the mystery of multiple maps. *J Comp Physiol A Neuroethol Sensory Neural Behav Physiol* 148: 287–296, 1982.
- Heiligenberg W, Partridge BL. How electroreceptors encode JAR-eliciting stimulus regimes: reading trajectories in a phase-amplitude plane. *J Comp Physiol A* 142: 295–308, 1981.
- Holt LL, Lotto AJ. Speech perception as categorization. *Atten Percept Psychophys* 72: 1218–1227, 2010.
- Hupé GJ, Lewis JE. Electrocommunication signals in free swimming brown ghost knifefish, *Apteronotus leptorhynchus*. *J Exp Biol* 211: 1657–1667, 2008.
- Hupé GJ, Lewis JE, Benda J. The effect of difference frequency on electrocommunication: chirp production and encoding in a species of

- weakly electric fish, *Apteronotus leptorhynchus*. *J Physiol (Paris)* 102: 164–172, 2008.
- Kara P, Reinagel P, Reid RC.** Low response variability in simultaneously recorded retinal, thalamic, and cortical neurons. *Neuron* 27: 635–646, 2000.
- Kawasaki M, Rose G, Heiligenberg W.** Temporal hyperacuity in single neurons of electric fish. *Nature* 336: 173–176, 1988.
- Knight BW.** Dynamics of encoding in a population of neurons. *J Gen Physiol* 59: 734–766, 1972.
- Kolodziejski JA, Sanford SE, Smith GT.** Stimulus frequency differentially affects chirping in two species of weakly electric fish: implications for the evolution of signal structure and function. *J Exp Biol* 210: 2501–2509, 2007.
- Krahe R, Bastian J, Chacron MJ.** Temporal processing across multiple topographic maps in the electrosensory system. *J Neurophysiol* 100: 852–867, 2008.
- Liberman AM, Mattingly IG.** A specialization for speech perception. *Science* 243: 489–494, 1989.
- Maler L.** Receptive field organization across multiple electrosensory maps. I. Columnar organization and estimation of receptive field size. *J Comp Neurol* 516: 376–393, 2009.
- Marsat G, Maler L.** Neural heterogeneity and efficient population codes for communication signals. *J Neurophysiol* 104: 2543–2555, 2010.
- Marsat G, Maler L.** Preparing for the unpredictable: adaptive feedback enhances the response to unexpected communication signals. *J Neurophysiol* 107: 1241–1246, 2012.
- Marsat G, Proville R, Maler L.** Transient signals trigger synchronous bursts in an identified population of neurons. *J Neurophysiol* 102: 714–723, 2009.
- May B, Moody DB, Stebbins WC.** Categorical perception of conspecific communication sounds by Japanese macaques, *macaca fuscata*. *J Acoust Soc Am* 85: 837–847, 1989.
- McKibben JR, Bass AH.** Behavioral assessment of acoustic parameters relevant to signal recognition and preference in a vocal fish. *J Acoust Soc Am* 104: 3520–3533, 1998.
- Metzner W, Juranek J.** A sensory brain map for each behavior? *Proc Natl Acad Sci USA* 94: 14798–14803, 1997.
- Meyer JH, Leong M, Keller CH.** Hormone-induced and maturational changes in electric organ discharges and electroreceptor tuning in the weakly electric fish *Apteronotus*. *J Comp Physiol A* 160: 385–394, 1987.
- Middleton JW, Longtin A, Benda J, Maler L.** Postsynaptic receptive field size and spike threshold determine encoding of high-frequency information via sensitivity to synchronous presynaptic activity. *J Neurophysiol* 101: 1160–1170, 2009.
- Moortgat KT, Keller CH, Bullock TH, Sejnowski TJ.** Submicrosecond pacemaker precision is behaviorally modulated: the gymnotiform electro-motor pathway. *Proc Natl Acad Sci USA* 95: 4684–4689, 1998.
- Narayan SS, Temchin AN, Recio A, Ruggero MA.** Frequency tuning of basilar membrane and auditory nerve fibers in the same cochleae. *Science* 282: 1882–1884, 1998.
- Nelken I, Rotman Y, Yosef OB.** Responses of auditory-cortex neurons to structural features of natural sounds. *Nature* 397: 154–157, 1999.
- Nelson DA, Marler P.** Categorical perception of a natural stimulus continuum: birdsong. *Science* 244: 976–978, 1989.
- Nelson ME, Xu Z, Payne JR.** Characterization and modeling of P-type electrosensory afferent responses to amplitude modulations in a wave-type electric fish. *J Comp Physiol A* 181: 532–544, 1997.
- Prather JF, Nowicki S, Anderson RC, Peters S, Mooney R.** Neural correlates of categorical perception in learned vocal communication. *Nat Neurosci* 12: 221–228, 2009.
- Pressley J, Troyer TW.** The dynamics of integrate-and-fire: mean versus variance modulations and dependence on baseline parameters. *Neural Comput* 23: 1234–1247, 2011.
- Salgado JA, Zupanc GK.** Echo response to chirping in the weakly electric brown ghost knifefish (*Apteronotus leptorhynchus*): role of frequency and amplitude modulations. *Can J Zool* 89: 498–508, 2011.
- Saul AB, Humphrey AL.** Spatial and temporal response properties of lagged and nonlagged cells in cat lateral geniculate nucleus. *J Neurophysiol* 64: 206–224, 1990.
- Siemers BM, Schnitzler HU.** Echolocation signals reflect niche differentiation in five sympatric congeneric bat species. *Nature* 429: 657–661, 2004.
- Silberberg G, Bethge M, Markram H, Pawelzik K, Tsodyks M.** Dynamics of population rate codes in ensembles of neocortical neurons. *J Neurophysiol* 91: 704–709, 2004.
- Simes RJ.** An improved Bonferroni procedure for multiple tests of significance. *Biometrika* 73: 751–754, 1986.
- Stamper S, Carrera-GE, Tan E, Fugère V, Krahe R, Fortune E.** Species differences in group size and electrosensory interference in weakly electric fishes: implications for electrosensory processing. *Behav Brain Res* 207: 368–376, 2010.
- Straka H, Vibert N, Vidal PP, Moore LE, Dutia MB.** Intrinsic membrane properties of vertebrate vestibular neurons: function, development and plasticity. *Prog Neurobiol* 76: 349–392, 2005.
- Tchumatchenko T, Malyshev A, Wolf F, Volgushev M.** Ultrafast population encoding by cortical neurons. *J Neurosci* 31: 12171–12179, 2011.
- Theunissen FE, Sen K, Doupe AJ.** Spectral-temporal receptive fields of nonlinear auditory neurons obtained using natural sounds. *J Neurosci* 20: 2315–2331, 2000.
- Todd B, Andrews D.** The identification of peaks in physiological signals. *Comput Biomed Res* 32: 322–335, 1999.
- Triefenbach F, Zakon H.** Changes in signalling during agonistic interactions between male weakly electric knifefish, *Apteronotus leptorhynchus*. *Anim Behav* 75: 1263–1272, 2008.
- van Hateren JH, Kern R, Schwerdtfeger G, Egelhaaf M.** Function and coding in the blowy h1 neuron during naturalistic optic flow. *J Neurosci* 25: 4343–4352, 2005.
- van Rossum MC.** A novel spike distance. *Neural Comput* 13: 751–763, 2001.
- Vernaleo BA, Dooling RJ.** Relative salience of envelope and fine structure cues in zebra finch song. *J Acoust Soc Am* 129: 3373–3383, 2011.
- Vinje WE, Gallant JL.** Sparse coding and decorrelation in primary visual cortex during natural vision. *Science* 287: 1273–1276, 2000.
- Vogel A, Hennig RM, Ronacher B.** Increase of neuronal response variability at higher processing levels as revealed by simultaneous recordings. *J Neurophysiol* 93: 3548–3559, 2005.
- Vonderschen K, Chacron MJ.** Sparse and dense coding of natural stimuli by distinct midbrain neuron subpopulations in weakly electric fish. *J Neurophysiol* 106: 3102–3118, 2011.
- Walz H, Hupé GJ, Benda J, Lewis JE.** The neuroethology of electrocommunication: how signal background influences sensory encoding and behaviour in *apteronotus leptorhynchus*. *J Physiol (Paris)* 107: 13–25, 2013.
- Wang X, Merzenich MM, Beitel R, Schreiner CE.** Representation of a species specific vocalization in the primary auditory cortex of the common marmoset: temporal and spectral characteristics. *J Neurophysiol* 74: 2685–2706, 1995.
- Zakon HH, Dunlap KD.** Sex steroids and communication signals in electric fish: a tale of two species. *Brain Behav Evol* 54: 61–69, 1999.
- Zakon HH, Oestreich J, Tallarovic S, Triefenbach F.** Eod modulations of brown ghost electric fish: JARs, chirps, rises, and dips. *J Physiol (Paris)* 96: 451–458, 2002.
- Zhang LI, Tan AY, Schreiner CE, Merzenich MM.** Topography and synaptic shaping of direction selectivity in primary auditory cortex. *Nature* 424: 201–205, 2003.
- Zupanc G, Maler L.** Evoked chirping in the weakly electric fish, *Apteronotus leptorhynchus*: a biophysical and behavioral analysis. *Can J Zool* 71: 2301–2310, 1993.
- Zupanc GK.** From oscillators to modulators: behavioral and neural control of modulations of the electric organ discharge in the gymnotiform fish, *apteronotus leptorhynchus*. *J Physiol (Paris)* 96: 459–472, 2002.